CHEMICAL ENGINEERING TRANSACTIONS
VOL. 106, 2023
A publication of AIDIC
The Italian Association of Chemical Engineering
Online at www.cetjournal.it
Guest Editors: Jeng Shiun Lim, Nor Alafiza Yunus, Peck Loo Kiew, Hon Huin Chin

ISBN 979-12-81206-05-2; **ISSN** 2283-9216
DOI: 10.3303/CET23106056

Facile Fabrication of Antimicrobial Zinc Ions Loaded Nanochitosan

Viet T. Tran, Chien Xuan Le, Hoa T. Ma, Tram Quynh Nguyen Truong, Nga H. N. Do, Phung K. Le*

Faculty of Chemical Engineering, Ho Chi Minh City University of Technology (HCMUT), VNU-HCM, Ho Chi Minh City, Vietnam
phungle@hcmut.edu.vn

Chitosan - the second most abundant polysaccharide on Earth has been known as a kind of non-toxic, environmentally friendly, biodegradable, antibacterial, and antifungal material. Compared with bulk chitosan-based materials, nanochitosan has superior properties in terms of permeability, solubility, and bioactivity. Nanochitosan is used as a carrier encapsulating various components via complexes with NH_2 and OH groups of chitosan molecules to protect, stabilize, and deliver targeted bioactive compounds. For the first time, chitosan-zinc ion nanoparticles (CSZ NPs) have been successfully synthesized by ultrasound-assisted ionic gelation to produce much smaller particles with enhanced antibacterial and antifungal activities. The fabricated CSZ NPs have a diameter from 119.3 to 212.6 nm, polydispersity index ranging from 0.2 to 0.3, and zeta potential from 16.4 to 22.4 mV. The average size of the as-fabricated CSZ NPs is two times smaller than zinc ions loaded nanochitosan without ultrasonic treatment. The spherical shape of the nanochitosan particles is confirmed, along with a wide range of elemental distributions, including C (29.74 %), O (42.14 %), Na (15.80 %), and Zn (1.11 %). The antimicrobial activities of CSZ NPs are evaluated by using the agar well diffusion method with gram-negative bacteria (*E. coli*, *P. aeruginosa*), gram-positive (*E. feacalis*, *S. aureus*, *S. aureus* methicillin-resistant (MRSA)), and fungi (*C. albicans*, *A. niger*). The minimum inhibitory concentration of CSZ NPs is 14 µg/mL for bacteria and more than 58 µg/mL for fungi. CSZ NPs have potential antimicrobial applications in the food industry and agriculture.

1. Introduction

Chitosan, a biological derivative of crustacean shells (shrimp, crab, oyster), fungi, and insect epidermis, has a chemical structure consisting of deacetylated D-glucosamine units linked via β-1,4-glycosidic linkages. Owing to its excellent film-forming properties, high adhesion ability, biodegradability, and effective antimicrobial properties, chitosan has been used in numerous applications, such as pharmaceuticals, food, agriculture, and biomedicine (Nga et al., 2022). In recent years, nanomaterials represent have become a highly efficient solution for diverse applications of in food processing, plant protection, water treatment, and biomedical sectors due owing to their extraordinary structural and physical properties, better solubility, and permeability, as well as greater bioactivities compared to the bulk materials. Nanochitosan can be synthesized by varied methods including ionic gelation, microemulsion, polyelectrolyte complexes, emulsification solvent diffusion, and reverse micellar. Taking advantage of the simplicity, high efficiency, and lack of consumption of toxic organic solvents, ionic gelation is mostly applied to produce nanochitosan (Hoang et al., 2022). Over the years, nanochitosan incorporated with plant extracts, essential oils, antibiotics, and metal ions has been effectively utilized as slow-release fertilizers, drug delivery systems, edible coating films, and antimicrobial agents to improve plant resistance (Divya et al., 2018). Many studies have been conducted on nanochitosan combined with metal ions consisting of Ag, Cu, Fe, and Zn ions for various applications (Hoang et al., 2022). Metal ions are widely used in food processing as mineral supplements, nutritional enhancers, and agricultural fertilizers due tobecause of their critical micronutrients for cell division, cell growth, immune function, enzyme activity, DNA synthesis, and protein production (Hoffmann et al., 2019). When the concentration is lower than the permitted limit, zinc ions

Paper Received: 23 May 2023; Revised: 24 July 2023; Accepted: 27 August 2023
Please cite this article as: Tran V.T., Le C.X., Ma H.T., Truong T.Q.N., Do N.H.N., Le P.K., 2023, Facile Fabrication of Antimicrobial Zinc Ions Loaded Nanochitosan, Chemical Engineering Transactions, 106, 331-336 DOI:10.3303/CET23106056

are of greater use due to their antimicrobial effects, low cost, non-toxicity, and essential ingredients for human health and plant systems.

Zinc ions combined with nanochitosan enhance the antimicrobial efficacy and have a potential application in the prevention of several plant diseases and food preservation. Dang et al. reported complexes of oligochitosan and zinc ions for inhibiting *Colletotrichum truncatum* fungus-caused anthracnose in chili peppers. The antifungal efficiency of the complex increases by 6-8 times compared than that of using oligochitosan alone, which is indicating its potential in controlling plant diseases (Dang et al., 2019). In addition, nanochitosan is used as a zinc ion carrier for grain farming applications, supplementing the micronutrients of seeds through foliar fertilization. The zinc content in seeds was significantly enhanced from 27 to 42 % when fertilized twice a week and extended to 5 weeks (Deshpande et al., 2017). Recently, ultrasonic technology has been considered one of the effective methods to reduce the size of nanoparticles and has been widely used in the synthesis of metal nanoparticles. The effect of ultrasonic waves on the dispersion of the active ingredients into a polymer matrix has been a primary matter issue in many studies.

Overall, the number of studies on the complex of nanochitosan and zinc ions is still limited, and these nanoparticles are only synthesized using a conventional ionic gelation method. The use of ultrasound in the synthesis process has not been extensively studied. This study presents a combination of nanochitosan and zinc ions (CSZ NPs) using an ionic gelation method assisted by ultrasound technology to effectively reduce the size of nanoparticles and enhance antimicrobial activities.

2. Experiment

2.1 Materials

Chitosan with a molecular weight of 158 kDa and a deacetylation degree of 75 % is obtained from Vietnam Food Joint Stock Company, Vietnam. Acetic acid (CH_3COOH, 99.8 %), zinc sulfate heptahydrate ($ZnSO_4.7H_2O$, 99.5 %), dimethyl sulfoxide (C_2H_6OS, 99.5 %), and sodium tripolyphosphate (STPP) ($Na_5P_3O_{10}$, 99.5 %) are purchased from Xilong Scientific Co., Ltd., Guangdong, China.

2.2 Preparation of zinc ions loaded nanochitosan (CSZ NPs)

The CSZ NPs are fabricated using ultrasound-assisted ionic gelation. Briefly, chitosan is dissolved in 1 % acetic acid by stirring for 1 h to obtain a final concentration of 0.3 % and then filtered to remove impurities. Subsequently, a homogenous mixture is obtained by mixing the chitosan solution and $ZnSO_4$ solution with different chitosan-to-zinc sulfate mass ratios (1:0.1, 1:0.3, 1:0.5, 1:0.7, and 1:1 w/w) with continuous stirring at 700 rpm. The STPP solution in distilled water is added dropwise to the mixture in a chitosan-to-STPP mass ratio of 1:0.4 w/w. Finally, the milky suspension of all ingredients is homogenized using a probe sonicator at 220 W for 10 min to prepare CSZ NPs.

2.3 Characterization of CSZ NPs

The dynamic particle size, polydispersity index (PDI), and zeta potential of the CSZ NPs are determined by using the Dynamic Light Scattering method at a scattering angle of 173 º (Malvern Zetasizer Nano ZS, UK) to study the stability of the system. The morphology of the CSZ NPs is determined using a JEOL JEM 1010 Transmission Electron Microscope (TEM) and elemental distribution by Energy Dispersive X-ray (EDX) analysis using S4800, Hitachi, Japan. The chemical characterization of CSZ NPs is confirmed using Fourier Transform Infrared spectroscopy (FTIR, Alpha II of Bruker, US) at wavenumber of 500-4,000 cm^{-1}. The crystalline and amorphous structures of CSZ NPs is identified by X-ray diffraction (XRD) using a D8 Advance, Bruker, US.

2.4 *In vitro* anti-microbial activity assay of CSZ NPs

The antibacterial and antifungal activities of CSZ NPs are studied investigated by using the agar well diffusion method. *Escherichia coli* (*E. coli)*, *Pseudomonas aeruginosa* (*P. aeruginosa)*, *Enterococcus faecalis* (*E. feacalis)*, *Staphylococcus aureus* (*S. aureus)*, and *S. aureus* methicillin-resistant (MRSA) bacteria are activated in tryptic soy agar. *Candida albicans* (*C. albicans)*, and *Aspergillus niger* (*A. niger)* in Sabouraud dextrose agar. The test medium, including Mueller-Hinton agar (MHA) for bacteria and 2 % glucose-added MHA for fungi is melted and poured into a petri dish to obtain the agar layers of 3-4 mm thickness. The microorganism density of activated bacteria and fungi is equivalent to 1-2.10^8 and 1-5.10^6 CFU/mL. The CSZ NPs sample is directly injected into the well on the medium at 50-60 µL per well. Amikacin and ketoconazole are used as positive controls. After incubation at 37 ºC for 24 hours, the diameter of the zone of inhibition for all samples is measured to evaluate the antimicrobial activity of CSZ NPs.

The minimum inhibitory concentration (MIC) of CSZ NPs against bacteria and fungi is determined by half-dilution of the initial concentration. The MHA medium is dispensed into test tubes with the correct volume to ensure uniform thickness of the agar plates, and autoclaved at 121 ºC for 15 min. The test substance is diluted with

dimethyl sulfoxide and directly mixed with the test medium to prepare a series of concentrations (20, 10, 5, 2.5, 1.25, 0.625, 0.32, 0.16, 0.08, 0.04, 0.02, 0.01, 0.005, and 0.0025 %). Positive and negative controls are prepared in the same manner.

3. Results and discussion

3.1 Particle size and zeta potential of CSZ NPs

As shown in Figure 1a, the kinetic diameters of the CSZ NPs gradually increased from 119.3 to 212.6 nm with an increase in the mass ratio of chitosan:Zn^{2+} from 1:0.1 to 1:1 (w/w). The PDI for size distribution increased from 0.25 to 0.32, but not significantly. Meanwhile, the zeta potential of CSZ NPs decreased from 22.4 to 16.4 mV (Figure 1b), which is attributed to the enhancement of complexes between the amine (NH_3^+) and hydroxyl (OH) groups of nanochitosan and Zn^{2+} ions. The presence of inter- and intramolecular interactions in CSZ NPs led to larger particle sizes, increased agglomeration, and reduced surface potential (Figure 2). This result differs from that of Deshpande et al., who reported that zinc-complexed chitosan nanoparticles had a higher zeta potential than empty nanochitosan (Deshpande et al., 2017).

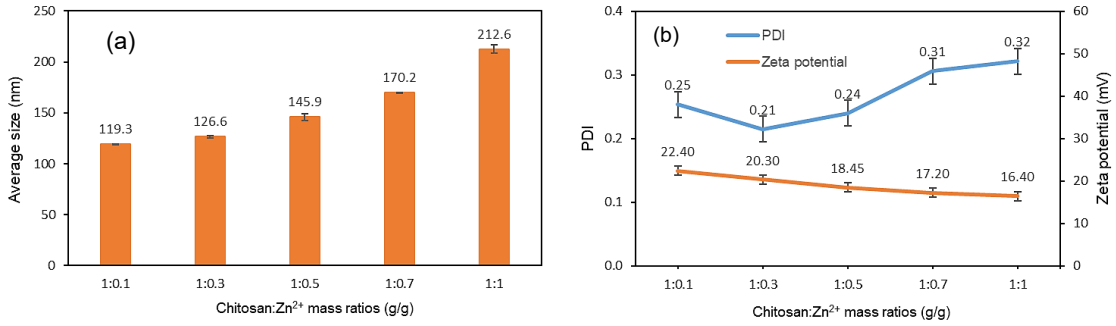

Figure 1: (a)Average size, (b) PDI and zeta potential of CSZ NPs with different mass ratios of chitosan:Zn^{2+} ratios (w/w).

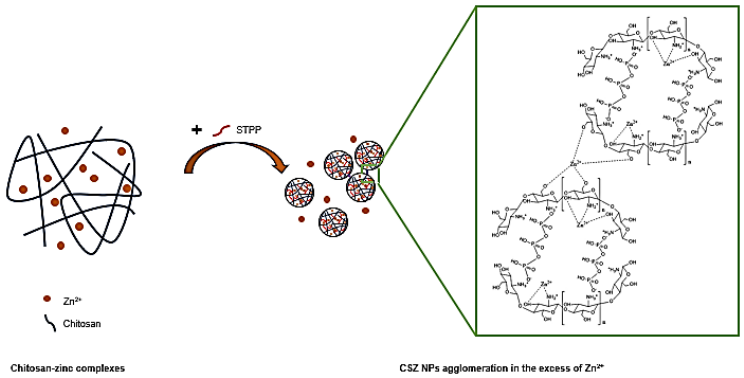

Figure 2: Formation and agglomeration mechanism of CSZ NPs in the excess of Zn ions.

3.2 Morphology of CSZ NPs

As shown in Figure 3, the morphologies of the nanochitosan and CSZ NPs is determined using TEM analysis. The nanochitosan and CSZ NPs have a spherical or oval shape, the diameter of nanochitosan distributes from 20-100 nm and CSZ NPs from 70-120 nm. These nanoparticles tend to agglomerate into larger sizes, and CSZ NPs are smaller compared with previous work of 200-300 nm (Choudhary et al., 2019) because of the effect of ultrasonic waves on the preparation of CSZ NPs, reducing their size significantly. Figure 4 shows the elemental analysis (EDX spectrum) of CSZ NPs. The strong peak at 1 keV represents sodium (15.80 %) in STPP and zinc (1.11 %) in $ZnSO_4$ (Patel et al., 2022). Other peaks detected in the spectrum are characteristic of sulfur (2.70 %) of $ZnSO_4$, phosphorus (4.49 %) of STPP, two elements of carbon (29.74 %), and oxygen (42.14 %), with major components characterized for chitosan (Hussain et al., 2020). In addition, chlorine and iron impurities have also been detected at 1.05 and 2.97 %. This indicates that zinc ions are mainly concentrated in the polymer structure of chitosan.

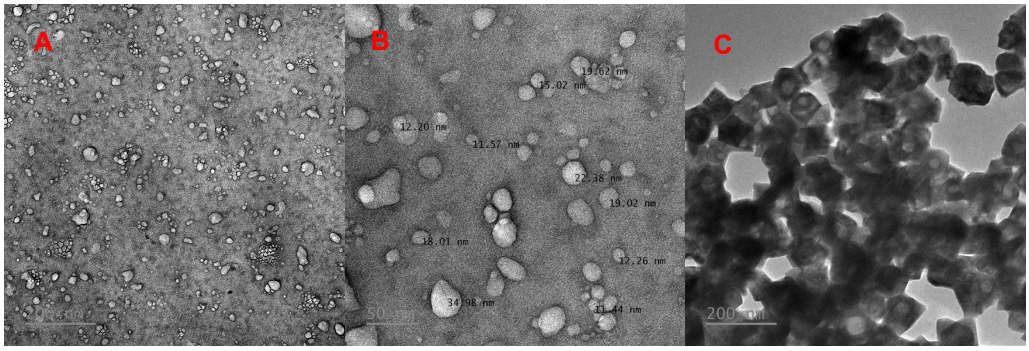

Figure 3: TEM images of nanochitosan (A, B) and CSZ NPs (C).

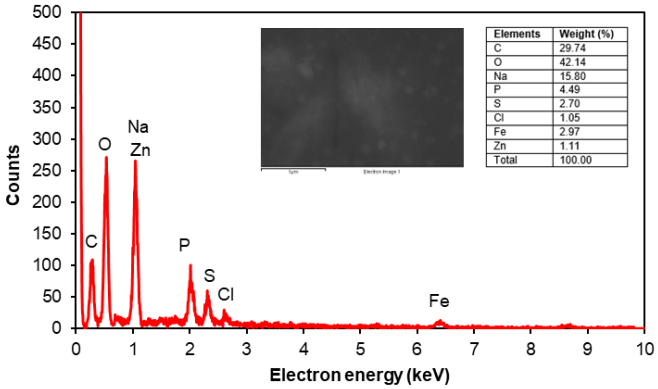

Figure 4: EDX spectrum of CSZ NPs (chitosan:Zn^{2+} of 1:0.1 w/w).

3.3 Chemical characterization of CSZ NPs

The chemical characteristics of pure $ZnSO_4$, nanochitosan, and CSZ NPs demonstrate through FTIR spectroscopy in Figure 5. For the salt spectrum, the oscillations at wavenumbers of 3,167, 1,662, 1,054, and 982 cm^{-1} are typical for the stretching vibration of the hydroxyl groups, at 1,662 cm^{-1} assigned to water, 1,054, and 982 cm^{-1} linked to SO_4 stretching (free sulfate groups) (Morais et al., 2021). Similar fluctuations from 2,918 to 3,356 cm^{-1} are observed for nanochitosan and CSZ NPs, which are typical for OH and NH_2 stretching vibration of amine groups present in chitosan molecules. The peaks at wavenumbers of 1,559 and 1,414 cm^{-1} in the spectrum of nanochitosan correspond to the C=O stretching vibration of the amide I group, which indicates the interaction between the amine group of chitosan and the polyanion group of sodium tripolyphosphate (OH et al., 2019). The similarity of the oscillation peaks of nanochitosan and CSZ NPs spectra may indirectly suggest that the zinc ion is loaded into the nanochitosan.

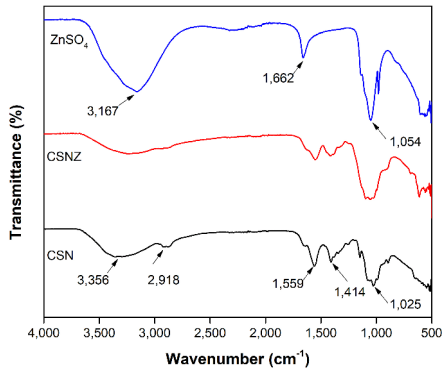

Figure 5: FTIR spectra of pure $ZnSO_4$, nanochitosan, and CSZ NPs.

3.4 XRD analysis of CSZ NPs

The XRD patterns of the chitosan, nanochitosan, and CSZ NPs are shown in Figure 6. Chitosan shows a crystalline structure with characteristic peaks at 2-theta of 10 and 20º, representing the (020) and (110) lattice planes. These two peaks in the spectra of nanochitosan and CSZ NPs are destroyed by the penetration of polyphosphate groups into the chitosan structure (Ali et al., 2018). The diffraction peaks recorded at 2-theta of 30º in the spectrum of CSZ NPs indicated the formation of a new crystalline phase in the nanochitosan structure upon zinc ions incorporation (El-saied et al., 2020).

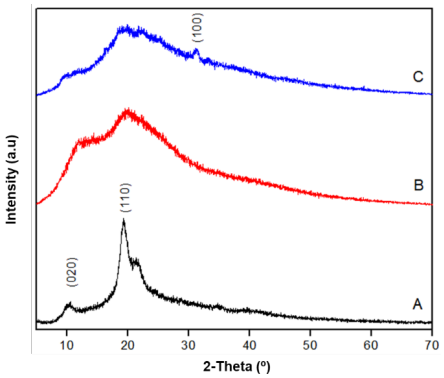

Figure 6: XRD spectra of chitosan (A), nanochitosan (B), and CSZ NPs (C)

3.5 *In vitro* antimicrobial activity assay of CSZ NPs

As shown in Table 1, zinc sulfate solution at the concentration of 882 µg/mL do not exhibit antibacterial and antifungal activities. Nanochitosan (2,250 µg/mL) has the poor antibacterial activity with inhibition zone of 9 mm and is not resistant to *C. albicans* and *A. niger* fungi. Meanwhile, CSZ NPs against most gram-negative and gram-positive bacteria have a diameter of 18–26 mm. The diameter of the MRSA bacterium obtained is 16 mm, which is equivalent to that of the antibiotic amikacin. CSZ NPs also showed resistance to *C. albicans* and *A. niger*, with diameters of 11 mm and 10 mm. The enhanced antibacterial properties of the zinc-chitosan complex can be attributed to several factors arising from the synergistic combination of zinc and chitosan, where the overall antibacterial activity of the complex is greater than their individual activities, involving multiple modes of action against microorganisms. Chitosan-zinc ion complexes can stabilize and control the release of zinc ions over time, ensuring prolonged exposure of microorganisms to the antimicrobial agent, thereby increasing the effectiveness of inhibiting bacterial growth. Furthermore, nanochitosan interacts with bacterial cell membranes and facilitates uptake of the complex into the cell. This enhanced cellular uptake allowed the complex to exert a more effective antibacterial activity. Zinc ions and chitosan may have different intracellular targets in bacterial cells and act on multiple sites simultaneously (Chandrasekaran et al., 2020).

Table 1: Diameter of the inhibition zone of pure $ZnSO_4$, nanochitosan, and CSZ NPs against bacteria and fungi (mm).

	E. coli	*P. aeruginosa*	*E. feacalis*	*S. aureus*	MRSA	*C. albicans*	*A. niger*
$ZnSO_4$ (882 µg/mL)	-	-	-	-	-	-	-
Nanochitosan (2,250 µg/mL)	9	9	9	-	9	-	-
CSZ NPs (2,250 µg/mL)	18	23	26	18	16	11	10
Amikacin	22	26	9	23	16	NA	NA
Ketoconazole	NA	NA	NA	NA	NA	22.3	26.8

NA: not applicable

Table 2 presents the MIC of CSZ NPs and the positive control, including the antibiotics amikacin and ketoconazole. CSZ NPs have found the amount of 14 µg/mL for inhibiting gram-negative (*E. coli, P. aeruginosa*), gram-positive (*E. feacalis, S. aureus*), and MRSA bacteria strains. Notably, this concentration is 18 times lower than that of the positive control for *E. faecalis*. CSZ NPs require a higher concentration of 58 µg/mL to inhibit *C. albicans* and *A. niger* fungi.

Table 2: MIC of CSZ NPs against bacteria and fungi (μg/mL).

	E. coli	*P. aeruginosa*	*E. feacalis*	*S. aureus*	MRSA	*C. albicans*	*A. niger*
CSZ NPs	14	14	14	14	14	> 58	> 58
Amikacin	2	4	256	4	8	NA	NA
Ketoconazole	NA	NA	NA	NA	NA	8	8

NA: not applicable

4. Conclusions

Zinc ion-loaded nanochitosan is successfully synthesized using ultrasound-assisted ionic gelation. The integration of ultrasonic waves into the CSZ NPs synthesis significantly reduced the particle size. CSZ NPs had an average size of 70-200 nm, PDI of 0.2-0.3, and high stability with a zeta potential of 16.4-22.4 mV. With their spherical shape, CSZ NPs show a high efficacy against gram-negative (*E. coli, P. aeruginosa*), gram-positive (*E. feacalis, S. aureus*, MRSA) bacteria, and *C. albicans, A. niger* fungi, caused disease in food processing. The MIC of CSZ NPs reached 14 μg/mL for bacterial strains and more than 58 μg/mL for fungi, which is 18 times lower than that of the antibiotic amikacin for *E. faecalis*. This study shows the potential applications of CSZ NPs in numerous fields, including food packaging, fertilizers, slow-release of zinc ions for plants, and the control of several diseases in human health.

Acknowledgment

We acknowledge Ho Chi Minh City University of Technology (HCMUT), VNU-HCM for supporting this study.

References

Ali M. E. A., Aboelfadl M. M. S., Selim A. M., Khalil H. F., Elkady G. M., 2018, Chitosan nanoparticles extracted from shrimp shells, application for removal of Fe (II) and Mn (II) from aqueous phases, Separation Science Technology 53(18), 2870-2881.

Chandrasekaran M., Kim K. D., Chun S. C., 2020, Antibacterial Activity of Chitosan Nanoparticles: A Review, Processes 8(9), 1173.

Choudhary R. C., Kumaraswamy R., Kumari S., Sharma S., Pal A., Raliya R., Biswas P., Saharan V., 2019, Zinc encapsulated chitosan nanoparticle to promote maize crop yield, International journal of biological macromolecules 127, 126-135.

Dang V. P., Bui D. D., Le N. A. T., Le T. H., Hoang D. H., Nguyen Q. H., 2019, Preparation and Antifungal Activity Investigation of Oligochitosan-Zn^{2+} on *Colletotrichum truncatum*, International Journal of Polymer Science 2019, 1-6.

Deshpande P., Dapkekar A., Oak M. D., Paknikar K. M., Rajwade J. M., 2017, Zinc complexed chitosan/TPP nanoparticles: A promising micronutrient nanocarrier suited for foliar application, Carbohydrate polymers 165, 394-401.

Divya K., Jisha M. S., 2018, Chitosan nanoparticles preparation and applications, Environmental chemistry letters 16(1), 101-112.

El-saied H. A.-a., Ibrahim A. M., 2020, Effective Fabrication and Characterization of Eco-friendly Nano Chitosan Capped Zinc Oxide Nanoparticles for Effective Marine Fouling Inhibition, Journal of Environmental Chemical Engineering 8(4), 103949.

Hoang N. H., Le Thanh T., Sangpueak R., Treekoon J., Saengchan C., Thepbandit W., Papathoti N. K., Kamkaew A., Buensanteai N., 2022, Chitosan Nanoparticles-Based Ionic Gelation Method: A Promising Candidate for Plant Disease Management, Polymers 14(4), 662.

Hoffmann T., Peters D., Angioletti B., Bertoli S., Péres L., Reiter M., De Souza C., 2019, Potentials Nanocomposites in Food Packaging, Chemical Engineering Transactions 75, 253-258.

Hussain M. S., Musharraf S. G., Bhanger M. I., Malik M. I., 2020, Salicylaldehyde derivative of nano-chitosan as an efficient adsorbent for lead(II), copper(II), and cadmium(II) ions, International journal of biological macromolecules 147, 643-652.

Morais E. G. d., Silva C. A., Jindo K., 2021, Humic Acid Improves Zn Fertilization in Oxisols Successively Cultivated with Maize–Brachiaria, Molecules 26(15), 4588.

Nga P. T. T., Nguyen H. P. N., Nguyen X. T., Pham T. P. M., Le P. T. K., 2022, A Mini-Review on Essential oils, Chitosan, and Their Application in Preserving Fruits and Vegetables, Chemical Engineering Transactions 97, 109-114.

OH J.-W., Chun S. C., Chandrasekaran M., 2019, Preparation and *In Vitro* Characterization of Chitosan Nanoparticles and Their Broad-Spectrum Antifungal Action Compared to Antibacterial Activities against Phytopathogens of Tomato, Agronomy 9(1), 21.

Patel M., Mishra S., Verma R., Shikha D., 2022, Synthesis of ZnO and CuO nanoparticles via Sol gel method and its characterization by using various technique, Discover Materials 2(1), 1.